Article

How Does the Electricity Demand Profile Impact the Attractiveness of PV-Coupled Battery Systems Combining Applications? †

Alejandro Pena-Bello [1,*] **, Edward Barbour** [2] **, Marta C. Gonzalez** [3,4,5] **, Selin Yilmaz** [1] **, Martin K. Patel** [1] **and David Parra** [1]

[1] Energy Efficiency Group, Institute for Environmental Sciences and Forel Institute, University of Geneva, Boulevard Carl-Vogt 66, 1205 Genève, Switzerland; Selin.Yilmaz@unige.ch (S.Y.); martin.patel@unige.ch (M.K.P.); david.parra@unige.ch (D.P.)

[2] Centre for Renewable Energy Systems Technology, Loughborough University, Loughborough LE11 3TU, UK; E.R.Barbour@lboro.ac.uk

[3] Department of City and Regional Planning, UC Berkeley, 406 Wurster Hall, Berkeley, CA 94720, USA; martag@berkeley.edu

[4] Lawrence Berkeley National Laboratory, Cyclotron Road, Berkeley, CA 94720, USA

[5] Department of Civil and Environmental Engineering and Engineering Systems, Massachusetts Institute of Technology, 77 Massachusetts Avenue, 1-290, Cambridge, MA 02139, USA

* Correspondence: alejandro.penabello@unige.ch

† This paper is an extended version of our paper presented in IRES 2019, Düsseldorf, Germany, 12–15 March 2019.

Abstract: Energy storage is a key solution to supply renewable electricity on demand and in particular batteries are becoming attractive for consumers who install PV panels. In order to minimize their electricity bill and keep the grid stable, batteries can combine applications. The daily match between PV supply and the electricity load profile is often considered as a determinant for the attractiveness of residential PV-coupled battery systems, however, the previous literature has so far mainly focused on the annual energy balance. In this paper, we analyze the techno-economic impact of adding a battery system to a new PV system that would otherwise be installed on its own, for different residential electricity load profiles in Geneva (Switzerland) and Austin (U.S.) using lithium-ion batteries performing various consumer applications, namely PV self-consumption, demand load-shifting, avoidance of PV curtailment, and demand peak shaving, individually and jointly. We employ clustering of the household's load profile (with 15-minute resolution) for households with low, medium, and high annual electricity consumption in the two locations using a 1:1:1 sizing ratio. Our results show that with this simple sizing rule-of-thumb, the shape of the load profile has a small impact on the net present value of batteries. Overall, our analysis suggests that the effect of the load profile is small and differs across locations, whereas the combination of applications significantly increases profitability while marginally decreasing the share of self-consumption. Moreover, without the combination of applications, batteries are far from being economically viable.

Keywords: PV; energy storage; battery; lithium-ion; combination of applications; clustering; load profile

1. Introduction and Literature Review

Rooftop photovoltaic (PV) systems have played a critical role in deploying solar energy owing to dramatic PV panel cost reductions (60% since 2010) driven by market-stimulating policies such as

feed-in tariffs (FiT), as well as ease of building integration and low maintenance [1,2]. As a result, batteries are increasingly being coupled to residential PV systems. The cost of batteries has also decreased by 65% since 2010 [1], with dedicated incentives in several locations [3].

Factors such as system size, location, electricity tariff structure, applications performed by the battery (also called services), PV generation and battery degradation impact the profitability of PV-coupled batteries. Most of these factors have already been addressed in the literature [4–9]. Overall, there is still a large variation in the value which a battery can offer to consumers across regions [10]. This variation can be partly explained by the household's electricity load profile [11], but this factor has received rather limited attention so far, in particular for batteries combining applications. Only for PV self-consumption, several authors have studied the impact of the household's load profiles. For example, Linssen et al. concluded that the profile has a significant impact on the optimal PV-coupled battery configuration after comparing three synthetic load profiles, different in terms of relation between peak and base load and load fluctuations, that were scaled to a single annual electricity consumption [12]. Schopfer et al. also highlighted that load profile is a key predictor of self-sufficiency and PV self-consumption according to the different machine learning models, and therefore key for taking PV-coupled battery investment decisions [11].

In the same way that the balance between PV generation and electricity demand influences self-consumption, it should influence the value of a PV-coupled battery performing other applications beyond PV self-consumption. However, earlier research on batteries performing multiple applications at the household level has not explored this yet. The review of O'Shaughnessy et al. found that apart from the total amount of electricity demand, the household's electricity load profiles determine the susceptibility to incentives for load shifting (using control of deferrable loads) but this review addresses exclusively studies with PV electricity as the sole input to the battery [13]. Among the literature focusing on the combination of applications, Ratnam et al. assessed the benefit of demand load-shifting for several households in Australia [14]. They found that in most of the cases, batteries performing demand load-shifting help to reduce the electricity bill.

Against this background, the present paper aims to contribute to an improved understanding of the impact of electricity load profile on PV-coupled batteries combining applications. To do so, we optimize the schedule of battery operation depending on considered applications, thereby including PV self-consumption, demand load-shifting, demand peak shaving and avoidance of PV curtailment, depending on the tariff structure. We focus on the impact of the load profile, annual consumption and combination of applications in two regions with very different climates, load profiles and electricity consumption, namely, Geneva (Switzerland) and Austin (US). We use a sizing ratio of 1:1:1 (e.g., an annual electricity consumption of 5 MWh leads to a nominal PV capacity of 5 kWp and a battery capacity of 5 kWh) which is commonly found in the literature (e.g., [4,15]).

The paper is structured as follows. The materials and methods are presented in Section 2 which describes the input data, the system configuration, electricity tariff design as well as the optimization setup and the techno-economic indicators. Section 3 gives the clustering and optimization results as a function of the combination of applications, clusters and location. Section 4 presents a discussion of the implications of our results and finally, Section 5 presents the main conclusions.

2. Materials and Methods

2.1. Demand Data

Two datasets of measured electricity demand from 305 dwellings in Austin (U.S., from the Pecan Street project) and 636 in Geneva (Switzerland) are used in this study, both with a temporal resolution of 15-minute throughout the year 2015. This temporal resolution provides a reasonable compromise between modeling technology performance and computational speed [16]. Figure 1 presents a normalized histogram (it shows the proportion of cases that fall into each of several categories, with the sum of the heights equaling 1) of the electricity demand data from Austin and

Geneva. Households in Austin have a median electricity consumption of 10.4 MWh p.a. (within a range of 2.9–23.9 MWh p.a.), while households in Geneva have a median electricity consumption of 2.5 MWh p.a. (within a range of 0.2–7.4 MWh p.a. In terms of average yearly electricity consumption the American households use 4.2 times more electricity than Swiss households from the datasets.
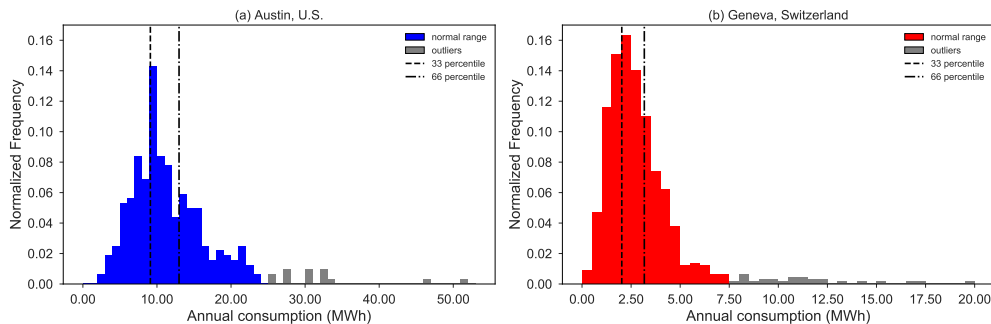

Figure 1. Normalized distributions of annual household electricity consumption for our data from (**a**) Austin, U.S. and (**b**) Geneva, Switzerland. Note that the scale of the horizontal axis differs for Geneva and Austin.

2.2. Load Profile Clustering

To generate representative consumer groups, we employ a clustering method. A range of clustering methods has been employed to form consumer segments in the previous literature (for a review of the clustering techniques applied to electricity load data see [17]). The k-means clustering method is one of the most widely used due to its versatility and applicability to large datasets [18–21]. Furthermore, it is important to normalize the smart meter data to identify time series with equivalent consumption patterns, instead of identical annual consumption [22,23]. While this approach is successful for forming groups of load profiles with similar shapes independent of consumption magnitudes, in this work we also need to study the effect of differing levels of overall consumption. Additionally, averaging the data suppresses the diversity of the electricity use patterns within the individual household. Therefore, it is important to find a robust analysis to identify clusters that explain the daily load profiles. Figure 2 shows the methodology used in this study to cluster and characterise the households in Geneva and Austin separately depending on the load patterns they exhibit, divided into four steps: segmentation by consumption level, normalization, clustering daily profiles and household classification.
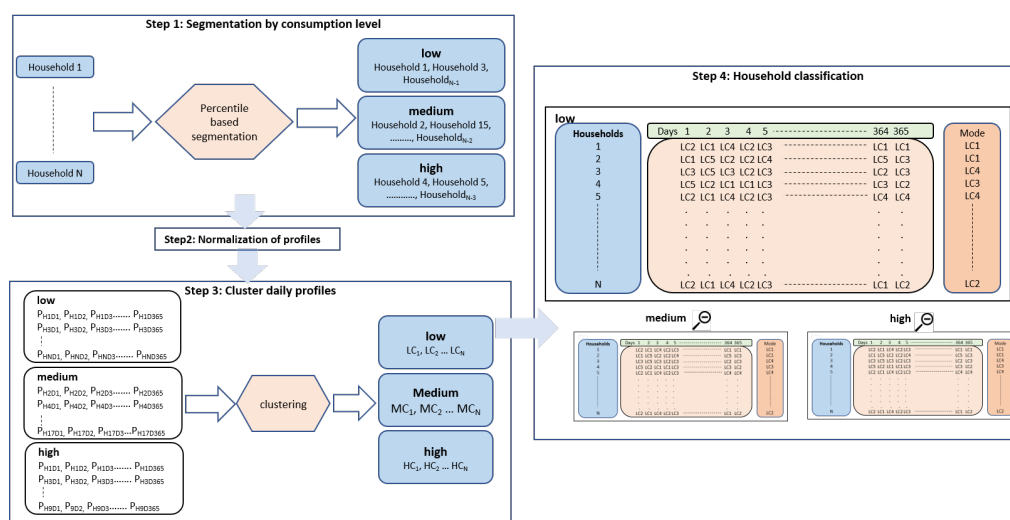

Figure 2. Methodological approach to electricity load profile characterisation through k-means clustering: Steps 1, 2, 3 and 4 are described.

Step 1 (segmentation by consumption levels): We first compare the distributions of annual consumption across both locations and form groups with similar consumption levels. Figure 1 shows that there are several non-representative consumers with abnormally high annual consumption which are excluded from the analysis. In particular, an annual consumption above 7500 kWh and 25,000 kWh is considered as an outlier in Switzerland and Texas respectively. We then split the remaining consumers into three separate groups—a low annual consumption group (0th–33rd percentile), a medium annual consumption group (34th–66th percentile) and a high annual consumption group in both locations (67th–100th percentile). Table 1 shows the boundaries of the categorization of yearly consumption levels for both Geneva and Austin.

Table 1. Consumption brackets per location.

Consumption Bracket	Austin (kWh p.a)	Geneva (kWh p.a.)
Low	[2900, 9052]	[150, 2025]
Medium	[9052, 12,365]	[2025, 3170]
High	[12,365, 24,000]	[3170, 7400]

Step 2 (normalization): We normalize the electricity load profiles in each sub-group (low, medium and high) in order to cluster the load profiles of the daily curves as described by Equation (1).

$$e_c(t) = \frac{l_c(t)}{\sum_{t=1}^{24} l_c(t)} \tag{1}$$

$e_c(t)$ is the normalized load at time t and $l_c(t)$ is the load of consumer c at time t before normalization.

Step 3 (clustering of daily profiles): We then cluster each daily profile within each sub-category of consumption levels (i.e., low, medium, high) as shown in Figure 2, where P_{HNDM} represents the daily profile of the household N at the day M. For example, if there are 50 households within the low consumption bracket in Geneva, the total number of profiles used for clustering corresponds to 18,250 (equivalent to 50 households × 365 days).

For clustering the normalized load profiles, we use the feature-based clustering, since it improves cluster quality relative to using raw profile data [23,24]. The principle of this approach is to extract few features to explain the shape of the load profile, thereby reducing the dimensionality of the time series (originally 15-minute data points) to avoid "curse of dimensionality", which refers to the fact that many algorithms become intractable when the input is high-dimensional [25]. Here, we focus on three key periods to analyze PV-coupled battery systems. First, we divide the daily profiles into three time periods based on the value of the mean load profile throughout the day: night-time (12 a.m.–10 a.m.), daytime (10 a.m.–6 p.m.) and evening time (6 p.m.–12 a.m.). It is important to note that cluster outcomes do not change if the periods are shifted by ±1 h based on the work of Yilmaz et al. [23] and Habner et al. [26]. The average values of the normalized profiles are calculated for each period, and they constitute the first three features to be included in the cluster analysis. The fourth feature corresponds to the mean standard deviation over the three periods, expressing variability in electricity demand throughout the day. By using the k-means clustering method, we randomly assign an initial set of centroids, and then move them in iterations to minimize the objective function given in Equation (2), which allows to identify the clusters. Here, j indexes the clusters from 1 to K and i indexes the load profiles assigned to the cluster j, where n_j is the total number of shapes in the cluster j. $e_{i,j}$ is the i-th load profile assigned to the cluster j and ζ_j is the centroid of the cluster j. Therefore, the Euclidean distance metric between centroids and the normalized load profiles (J) is minimized. Finally, f is the feature index.

$$J = \sum_{j=1}^{K} \sum_{i=1}^{n_j} \sqrt{\sum_{f=1}^{f=4} (e_{i,j}(f) - \zeta_j(f))^2} \tag{2}$$

The silhouette score (*s*) presented by Rousseeuw [27], defined in Equation (3), is used to determine the optimal value for the number of clusters (*k*), where *a* is the average intra-cluster distance, and *b* is the average shortest distance to another cluster. Consequently, the silhouette score has a range of $[-1, 1]$, where a score close to +1 indicates a better performance of the clustering algorithm. The algorithm that produces clusters with low intra-cluster distances (i.e., high intra-cluster similarity) and high inter-cluster distances (i.e., low inter-cluster similarity) has a high silhouette score. The *k* with the highest silhouette score corresponds to the optimum number of clusters for each consumption group.

$$s = \frac{b - a}{max(a, b)} \tag{3}$$

Step 4 (household classification): We then list the cluster IDs that each household exhibit on a particular day for the whole year. As households use electricity differently on a daily basis, there are multiple cluster IDs over a period. We, therefore, used the statistical mode of the cluster outcome to determine the most common cluster ID for each household throughout the year, and classify that household with the corresponding ID.

2.3. PV Generation

Outdoor temperature and horizontal solar irradiance monitored in both locations for the year 2017 are used to model PV generation. Hourly solar irradiation and temperature data from Austin, Texas was obtained from the National Solar Radiation Database provided by NREL (https://nsrdb.nrel.gov/, accessed on 20 July 2020), as for Geneva, the data was collected by the UNIGE (http://www.cuepe. ch/html/meteo/archives-numeriques.html, accessed on 20 July 2020). We simulate PV generation using a standard one-diode model [28] and PV technology with a nominal efficiency of 18.6% [29], representative of the current state. The model also includes a maximum power point tracker system, as is the case of most PV systems in order to maximize the output regardless of the environmental conditions (temperature and solar irradiance). The installed capacity of the PV system is modeled based on the annual demand of each household with 1 kWp installed per 1 MWh of annual demand (i.e., 1000 full-load hours) [15].

2.4. PV-coupled Battery System

We analyze the techno-economic implications of adding a battery system to a new PV system that would otherwise be installed on its own (we hereby disregard all costs related to the PV system). We assume a DC-coupled configuration illustrated in Figure 3, including an integrated inverter with a buck-boost charge controller (i.e., a step-up and step-down converter combined), a maximum power point tracking system and a bi-directional inverter (required to charge a battery from the main grid). An inverter loading ratio (i.e., the ratio between the inverter rating and the PV rating, referred to as ILR) of 1.2 is considered for this study [30]. We simulate Lithium Nickel Manganese Cobalt Oxide (NMC) batteries since this technology is currently dominating the residential market. The battery capacity is coupled to the PV system in a one-to-one ratio, i.e., 1 kWh battery capacity per 1 kWp of PV installed. Following a conservative approach, we consider relatively high installation costs for the battery and inverter, equal to 2000 USD in both countries, regardless their nominal capacity [31]. We assume that NMC batteries can use 100% of depth of discharge (DoD) [32] and can be charged or discharged in 2.5 h (i.e., a C-rate of 0.4* C, where C is the nominal capacity of the battery). Moreover, we consider the battery to reach the end-of-life (EoL) when 30% of the nominal capacity is depleted [33]. The techno-economic values for the PV-coupled battery system used in this study are displayed in Table 2.
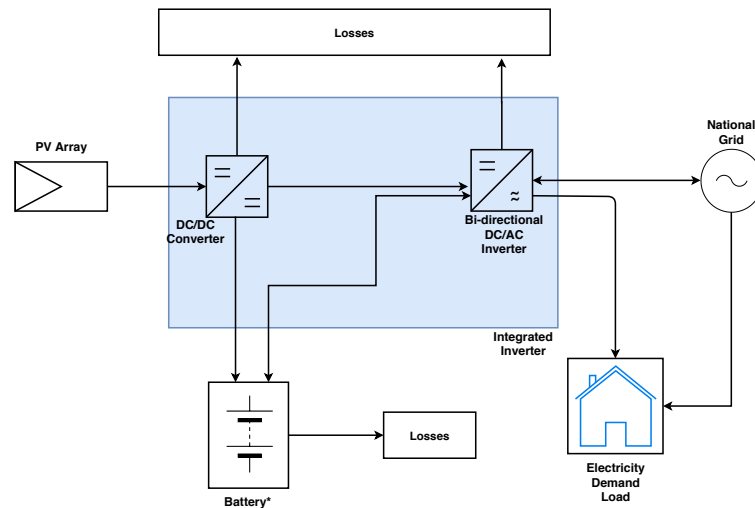
Figure 3. DC-coupled PV-battery system with integrated inverter used in this study. Arrows indicate the direction of possible energy flows between the individual components.

Table 2. Values selected for the technical and economic assessment of PV-coupled battery systems. The cycle aging factor is given for a 100% depth-of-discharge.

Component	Units	Value	Reference
Charge controller efficiency	%	98	[34]
Inverter efficiency	%	94	[34]
Bi-directional inverter cost	USD/kW	600	[35]
Bi-directional inverter lifetime	years	15	[36]
Balance of plant cost	USD/kW	100	[6]
Installation costs	USD	2000	[31]
O&M	USD/kW	0	[37]
Discount factor	% p.a.	4	[38]
End of life (EoL)	%	70	[39]
ILR	p.u.	1.2	[30]
Cycles at a given depth of discharge	-	5000 @ 100%	[37]
Battery lifetime	Years	15	[37]
Battery roundtrip efficiency	%	91.8	[37]
Battery Energy costs	USD/nominal kWh	410	[37]
Maximum charge/discharge rate	kW	0.4*C	[37]
ΔSOC	%	100	[32]
Maximum SOC	%	100	[32]
Minimum SOC	%	0	[32]
Cycle aging factor	per cycle	0.00042	Based on [7]
Calendar aging factor	per day	0.00038	Based on [7]

2.5. Electricity Tariff Design and Battery Applications

In this study, we consider all battery applications which help consumers to reduce their bill, namely PV self-consumption, avoidance of PV curtailment, demand load-shifting and demand peak shaving, except for back-up power. Back-up power is excluded since we focus on distribution areas with a high level of grid stability. These consumer applications can be described as follows (see also [40]): PV self-consumption, the predominant application for residential batteries, uses the battery to store PV surplus electricity for later consumption. Avoidance of PV-curtailment applies where grid regulators seek to maintain grid stability through feed-in limitations, prohibiting injection of PV power into the grid above a threshold level. The PV excess is stored in the battery and can be used at a later time, thereby allowing to increase the share of renewable energy used. Demand load-shifting uses the battery to exploit varying tariff differentials, shifting electricity consumption to times with low price. Finally, demand peak-shaving uses energy stored in the battery to reduce

the maximum power drained from the grid (in kW) in order to mitigate demand electricity peaks. These various applications are enabled by different retail electricity tariff structures.

Demand-peak shaving is performed if, in addition to a a volumetric component (USD/kWh), the retail tariff also includes a capacity-based tariff (USD/kW) to bill the peak demand. Capacity tariffs are being widely suggested following the penetration of air conditioning, heat pumps and electric vehicles [41]. In order to ensure that the tariffs are on average revenue neutral for all the households evaluated (i.e., the utility company does not charge more money for the same service and the consumer bill remains in a similar range), the per-kWh rates are reduced by 20% and 30% in Geneva and Austin respectively, whenever the capacity-based tariff is assumed. Additionally, currently where capacity tariffs are in place (typically for higher voltage consumers) volumetric charges are lower.

For the volumetric component, we also compare a flat tariff, for which the battery only performs PV self-consumption, and a double tariff (also referred to as a Time-of-use tariff), for which demand load-shifting is also performed. Based on the current offer from local utilities, the double tariff is applied throughout the year in Geneva, but only in summer-time in Austin. Finally, a (physical) feed-in limit of 50% of the PV nominal capacity (i.e., a user cannot inject PV electric power beyond 50% of its PV rated power into the grid) is assumed in order to prevent instability on the power system, which is a main concern during periods with large PV production periods, following the example of Germany [8]. This allows a PV-coupled battery to get some value by avoiding PV curtailment.

Based on the sharp decline of FiT across many countries, the PV export price is assumed to correspond to the wholesale electricity price, as is the case for traditional electricity generators. Wholesale electricity prices from the day-ahead market for Texas (from ERCOT southern load zone, average price of 0.027 USD/kWh) and Switzerland (from EPEXSPOT, average price of 0.047 USD/kWh) are used. Table 3 displays the values of the electricity tariff used in this study. It is important to highlight that electricity bills include also other fixed costs, such as taxes and grid usage.

Table 3. Electricity tariff components depending on the bill structure used in this study. The peak time in Geneva occurs from 7:00 to 22:00 on weekdays and from 17:00 to 22:00 for the weekends, whereas it is from 13:00 to 19:00 for the weekends between June and September in Austin. The PV export price corresponds to the wholesale price, with the given value corresponding to the average wholesale price.

Name		Units	U.S.	Switzerland	Based on
Flat Tariff		USD/kWh	0.07	0.22	Energy
Double Tariff	On-peak	USD/kWh	0.18	0.24	Energy
	Off-peak	USD/kWh	0.06	0.15	Energy
Export price		USD/kWh	0.03	0.05	Energy
capacity-based tariff		USD/kW/month	10.14	9.39	Power
Feed-in limit		$\% kW_{p-PV}$	50%	50%	Power

2.6. Optimization of the Battery Schedule

The management problem of a PV-coupled battery system is solved using the open-source model presented in [33], which relies on Pyomo, an open-source tool for modeling optimization applications in Python [42] and is solved with CPLEX. The battery schedule is optimized on a daily basis (i.e., 24 h optimization framework, with a resolution of 15-minute) and we assume perfect day-ahead forecast of the electricity load profile, solar PV generation and wholesale prices in order to determine the maximum economic potential regardless of the forecast strategy used. Aging of the battery was treated as an exogenous parameter, calculated on a daily basis, and therefore not subject to optimization (for further information see [33]).

The objective function, Equation (4), minimizes the costs C incurred by the households, thereby considering two components, namely the energy and power components of the electricity bill. The energy component is composed of the costs of electricity imports and the reward for the electricity exports. The power component relates to the maximum power used by the household. Here, i is

the time of the day, E_{grid} is the energy drained from the grid, $E_{PV-grid}$ is the energy exported to the grid, π_{import_i} is the import price, π_{export_i} is the export price, $P_{max-day}$ is the maximum power at each day, $\pi_{capacity}$ is the capacity price (USD/kW/day) and *PS* is a Boolean parameter to activate the power-based factor of the bill when necessary.

$$C = min(\overbrace{\sum_{i=0}^{t}(E_{grid_i} \cdot \pi_{import_i} - E_{PV-grid_i} \cdot \pi_{export_i})}^{\text{Energy-based tariff}} + \underbrace{(P_{max-day} \cdot \pi_{capacity} \cdot PS)}_{\text{Power-based tariff}})) \quad (4)$$

For further information on the constraints, parameters and validation of the model please see [33]. The model and the U.S. data (the Swiss data is confidential) are publicly available in https://github.com/alefunxo/Basopra (accessed on 20 July 2020).

Every optimization is run for one year and then the results are linearly extrapolated to cover the PV's entire lifetime (i.e., 30 years). We assume 30% of capacity depletion as the battery's end-of-life [43] and assume replacements of inverter and battery, in the case that the (replacement) battery lifetime exceeds the project lifetime, the residual value of the battery is considered using straight-line depreciation [44]. We take a conservative approach maintaining the same battery cost for the future (discounted to the present), due to the high uncertainty linked to future battery costs. The analysis is conducted with identical electricity prices for all years across battery lifetime.

2.7. Techno-Economic Indicators

We use three indicators to compare the impact of the household's load profile on the attractiveness of the PV-coupled battery systems. As technical indicators, we use (i) the PV self-consumption (SC), which is the share of on-site generation that is auto-consumed (Equation (5)), which is the most relevant indicator for prosumers who pursue autarky. Although in this study all the applications provided by the battery deliver power exclusively to the household, it is noteworthy to mention that in the case that the battery is used to provide electricity to the grid for additional applications (e.g., frequency control), this energy should not be accounted for self-consumption. (ii) The maximum peak flow shaved (PS) in the electricity exchange with the grid (Equation (6)), taking into account both import and export power flow, is a very relevant for distribution grid planning. In addition, we use (iii) the Net Present Value (NPV) to quantify the battery investment attractiveness, which is relevant for prosumers from a financial point of view (see Equations (7) and (8)). The NPV is calculated using annual project cash flows (CF) taking into account the difference between the cash flows from a PV-coupled battery system and a system with only PV.

$$SC = \frac{\sum_{i=0}^{N}(E_{PV-total-demand} + E_{PV-batt-demand})}{\sum_{i=0}^{N} E_{PV}} \quad (5)$$

$$PS = \frac{P_{grid-batt} - P_{grid-nobatt}}{P_{grid-nobatt}} \quad (6)$$

$$CF_{Batt_i} = CF_{PV-Batt_i} - CF_{PV_i} \quad (7)$$

$$NPV = \sum_{i=1}^{N} \frac{CF_{Batt_i}}{(1+r)^i} - \sum_{i=0}^{N} \frac{CAPEX}{(1+r)^i} \quad (8)$$

In Equation (5), $E_{PV-total-demand}$ is the PV generation used to meet the household demand, $E_{PV-batt-demand}$ is the energy from the PV that is charged into the battery and delivered to the household demand and E_{PV} is the total PV generation. In Equation (6), $P_{grid-batt}$ is the peak flow exchanged with the grid with a battery and $P_{grid-nobatt}$ is the peak flow without a battery (i.e., only

with a PV system). $CF_{PV-Batt_i}$ is the cash flow of the PV-coupled battery system, CF_{PV_i} is the cash flow of the PV system alone and CF_{Batt_i} is the cash flow due to the installation of the battery system in Equation (7). Finally, $CAPEX$ represents the total capital expenditures (excluding the PV system), *r* is the discount factor (a weighting term that multiplies value to discount it back to the present value), *i* is the year and *N* is the lifetime of the project in Equation (8).

3. Results

We firstly present the clustering results, then the technical results and finally, the NPV for PV-coupled systems as a function of the load profile, the electricity consumption bracket (i.e., low, medium or high electricity consumption) and the location (namely Austin and Geneva). We assess three combinations of applications. First, a baseline scenario, where PV self-consumption is analyzed individually (using a flat tariff). Secondly, PV self-consumption is combined with demand peak-shaving (using a flat tariff and a capacity-based tariff), since it is reported to be the next most attractive application for residential consumers (see [39,41]). Finally, the combination of PV self-consumption, demand peak shaving (using a capacity-based tariff), demand load-shifting (using a Time of Use -ToU- tariff, structured according to peak and off-peak times of day) and avoidance of PV curtailment (using a physical feed-in limit). To highlight the statistically significant differences across the results, a Shapiro-Wilk test is used to prove non-normality of the results, followed by a paired Wilcoxon test with Holm procedure to control the family-wise error rate. We report the p-values that indicate the probability of obtaining test results at least as extreme as the results actually observed, assuming that the null hypothesis is correct.

3.1. Clustering Results

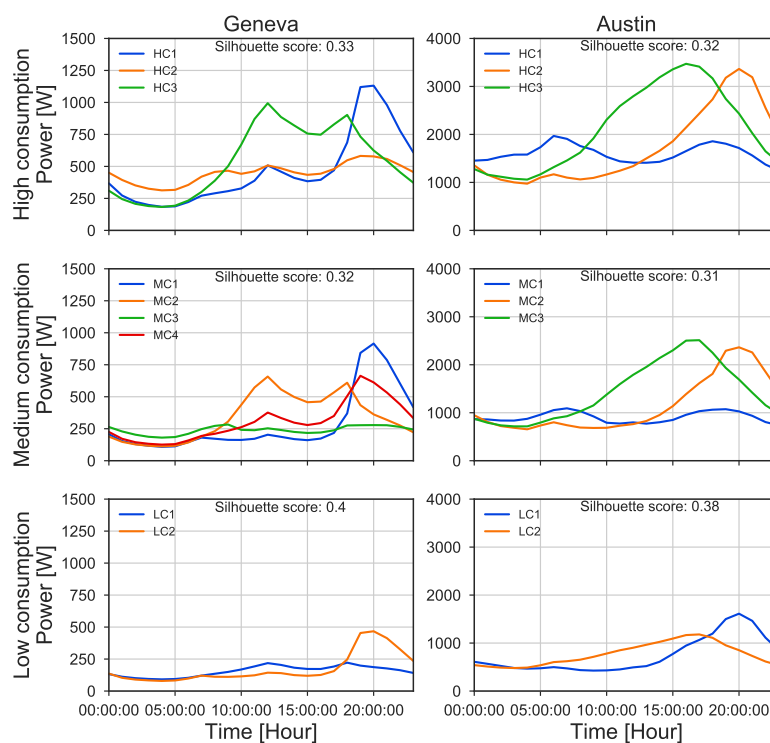Table 4 presents the distribution of cluster IDs (i.e., the statistical mode of daily profiles) for each consumption level and location, including number and percentage of households. Figure 4 shows the cluster centroids for daily electricity load profiles with their average silhouette score for each sub-group and location. In Geneva two clusters with similar shape are present across the three consumption brackets, one with a high peak in the evening and one that is mostly flat. In Austin, there are as well two similar clusters across the three consumption brackets with one high peak around 16 h, the second one presents a high peak around 20 h. The optimal number of clusters k for each approach was determined based on the highest silhouette score. The silhouette analysis, displayed in Figure 5, shows the optimum number of clusters for each combination of location and consumption bracket: *k* = 2 for Texas-low; *k* = 3 for Texas-medium; *k* = 3 for Texas-high; and *k* = 2 for Geneva-low; *k* = 4 for Geneva-medium; *k* = 3 for Geneva-high. The silhouette scores improve as more aggregation/averaging of profiles is applied, with the best scores resulting from aggregating each day across all households and the worst scores for the approach without aggregation (here in this paper we cluster one profile per household per day hence silhouette scores are slightly lower than those published in literature for average profiles).

Table 4. Cluster nomenclature by consumption bracket and location. The assignation of every household depends on the statistical mode of the cluster outcome to determine the most common cluster ID throughout the year.

Consumption Bracket	Geneva		Austin	
	Cluster ID	**Number of Households** (%)	**Cluster ID**	**Number of Households (%)**
Low	LC1	177 (27.8%)	LC1	14 (4.6%)
	LC2	43 (6.8%)	LC2	86 (28.2%)
Medium	MC1	14 (2.2%)	MC1	24 (7.9%)
	MC2	63 (9.9%)	MC2	16 (5.2%)
	MC3	57 (9.0%)	MC3	60 (19.7%)
	MC4	86 (13.5%)	-	-
High	HC1	54 (8.5%)	HC1	16 (5.2%)
	HC2	71 (11.2%)	HC2	26 (8.5%)
	HC3	71 (11.2%)	HC3	63 (20.7%)

Figure 4. Centroids of the various clusters found for daily electricity profiles with their average silhouette score for each sub-group and location. Note that the scale of the vertical axis differs for Geneva and Austin.
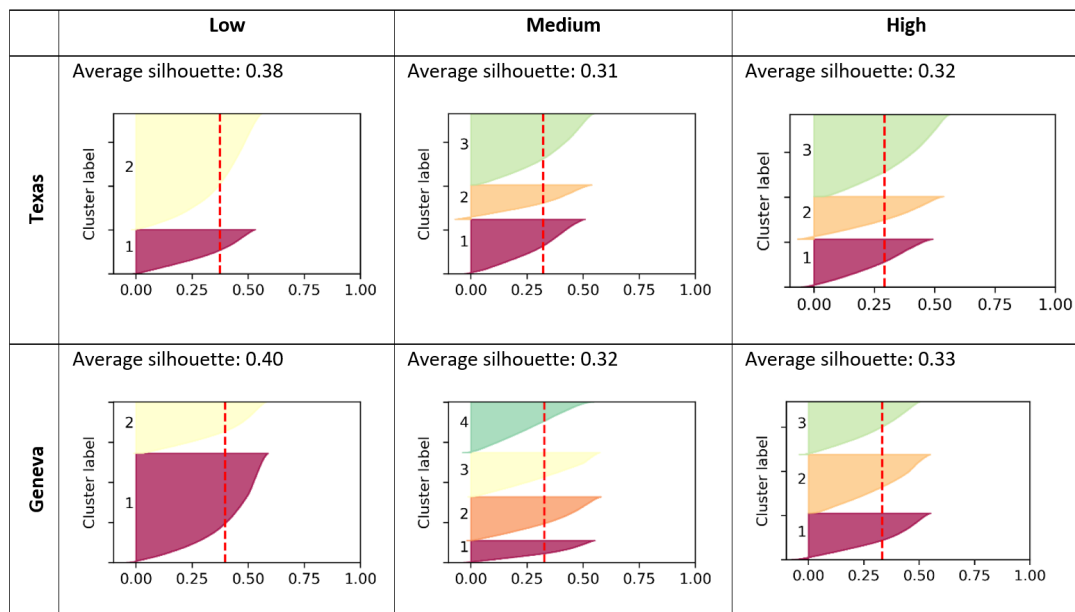
Figure 5. Silhouette analysis for k-means clustering using the daily profile features (optimum number of clusters, k = 2 for Texas low; k = 3 for Texas-medium; k = 3 for Texas-high and k = 2 for Geneva low; k = 4 for Geneva-medium; k = 3 for Geneva-high).

3.2. PV Self-Consumption

The increase of PV self-consumption share due to addition of a battery to the PV system ranges between 14–22% in Austin and 6–24% in Geneva, with median values of 19% and 18%, respectively as shown in Figure 6a. Regarding the combination of applications, there is a slight reduction (2.6%) of the total PV self-consumption in the households in Austin when other applications are performed together with PV self-consumption (p-value < 0.05). However, this is not the case for the households in Geneva, which may suggest that there is no competition among applications as is the case in Austin.

Regardless the combination of applications, the PV self-consumption increases with electricity consumption in both countries (p-value < 0.05). However, this increase is small, with median differences between the low and high consumption brackets of only 2% and 3% for Austin and Geneva, respectively (see Figure 6b). The load profile influences PV self-consumption (p-value < 0.05) and it can differ by up to 5% (e.g., LC1 vs. LC2 in Austin, see Figure 6c), while it is more limited when comparing households with a peak during daytime (dashed boxplots in Figure 6c,d, e.g., MC2 and HC3 in Geneva) with those without a daytime peak, with maximum median differences of 4% and 2.5% for Austin and Geneva, respectively. Overall, the addition of a battery significantly increases the self-consumption, especially for households with a peak during daytime; the low penalty related to combining all applications suggests that it is a smart strategy to follow.
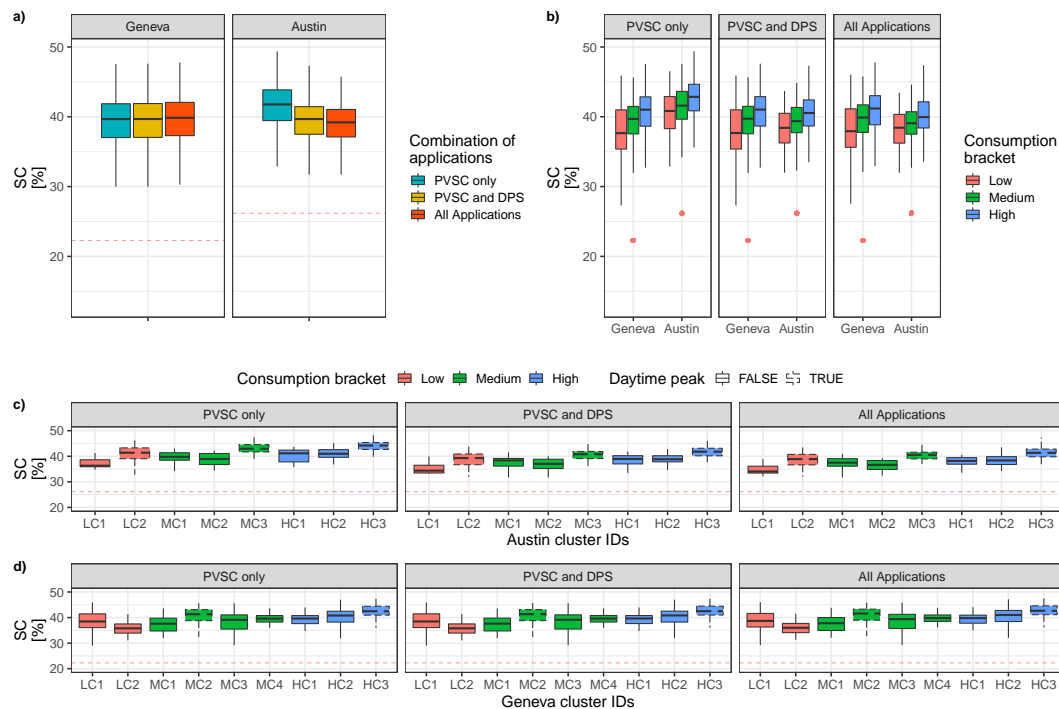
Figure 6. PV self-consumption (SC) of PV-coupled batteries. (**a**) Comparing the impact of the combination of applications per country; (**b**) Comparing the consumption bracket impact per country and per combination of applications; (**c**) Comparing the impact of the load profile (cluster) per consumption bracket and per combination of applications for Austin and; (**d**) Comparing the impact of the load profile (cluster) per consumption bracket and per combination of applications for Geneva. Dashed boxplots represent households with peaks during daytime (i.e., from 10 a.m. to 6 p.m.). The number of observation per cluster is indicated on top of the boxplots. The red dashed lines and red points represent the median SC of the same PV system without battery support. PVSC stands for PV self-consumption and DPS for demand peak shaving.

3.3. Peak Shaving

Figure 7 shows the results of peak flow reduction in absolute terms for PV-coupled battery systems, for the three combination of applications we analyze. In the case of PV self-consumption only, there is not incentives to reduce the peak (i.e., no capacity-based tariff) and therefore, the peak in some cases can be even higher than the case where PV systems are installed without a battery (i.e., 0 kW of peak shaved). The combination of PV self-consumption and demand peak shaving reduces the median peak flow by 1.9 kW and 1.1 kW in Austin and Geneva, respectively, when compared to the cases where the battery is used exclusively for PV self-consumption (see Figure 7a, p-values < 0.05). Additionally, when demand load-shifting (allowance to charge from the grid) and avoidance of PV curtailment are included on top of the above mentioned applications (i.e., when all applications are combined), the median peak flow is reduced further by 1.5 kW in Austin and 0.1 kW in Geneva, compared to the PV self-consumption and demand peak shaving combination (p-values < 0.05). In total, peak flow reduction by up to 3.4 kW and 1.2 kW can be achieved in Austin and Geneva, respectively, which compared to the median value of the maximum power demand across both datasets (7.9 kW and 3.8 kW), represents a substantial reduction of peak flow.

The peak flow reduction when there are incentives to reduce it, is moderately affected by the annual consumption of the household (see Figure 7b). For instance, the median values of the peak flow are reduced more in households with high electricity consumption than in households with low electricity consumption when all applications are combined; for high electricity consumption households, it is reduced by up to 5.1 kW in Austin and up to 1.6 kW in Geneva, whereas the maximum

reduction for low electricity consumption households amounts to 2.5 kW and 0.6 kW in Austin and Geneva, respectively.

The impact of the load profile on the peak flow reduction achieved by batteries in Austin is in general not statistically significant. The only case where there is a statistically significant difference is when all applications are combined (i.e., right panel in Figure 7c), and the median values between households with peaks in the evening (HC2) and with a peak during daytime (HC3) are compared, with a median difference of 2.2 kW. For Geneva (Figure 7d), when PV self-consumption is combined with demand peak shaving, the peak flow reduction in households with medium annual demand and a flat load profile (MC3) is slightly lower (0.1 kW of difference, *p*-value < 0.05) than in households with a demand peak during daytime (MC2) or with double demand peak (one during the day and one in the evening, MC4). Similarly, in houses with high annual electricity demand, the differences between the households with a flat load profile (HC2) and other households is small in power terms (0.3 kW, *p*-value < 0.05). When all applications are combined, the differences between the households presenting a flat load profile and those with a peak in the evening (HC1) are no longer statistically different. The absence of statistically significant differences among the different clusters (but within consumption brackets) suggest a low impact of the load profile on the peak flow.
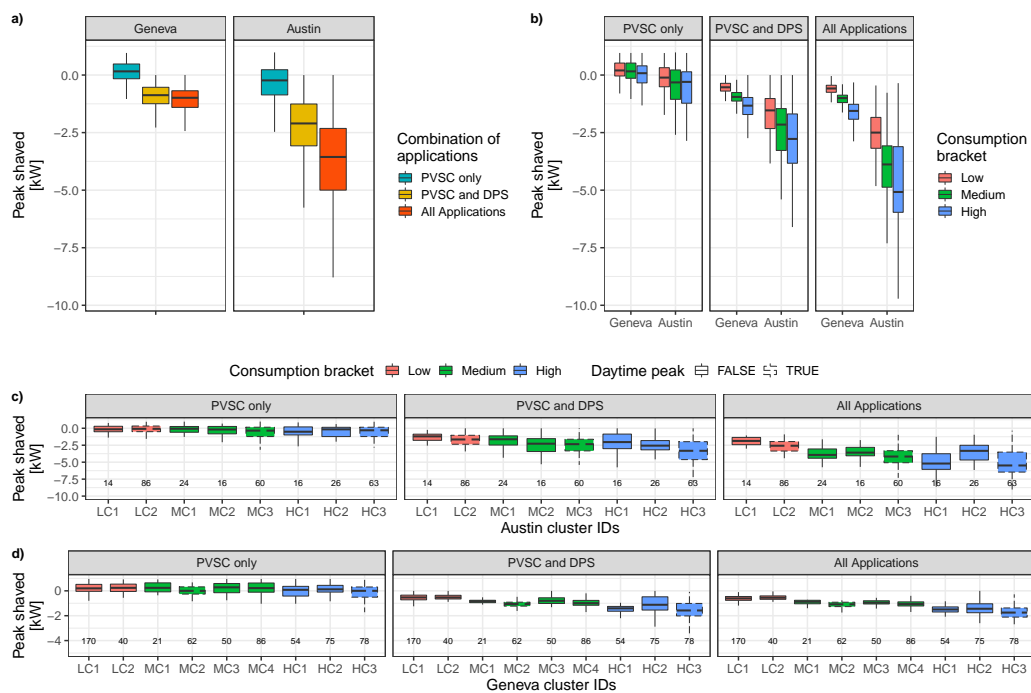

Figure 7. Peak flow shaved by PV-coupled batteries. (**a**) Comparing the impact of the combination of applications per country; (**b**) Comparing the consumption bracket impact per country and per combination of applications; (**c**) Comparing the impact of the load profile (cluster) per consumption bracket and per combination of applications for Austin and; (**d**) Comparing the impact of the load profile (cluster) per consumption bracket and per combination of applications for Geneva. Dashed boxplots represent households with peaks during daytime (i.e., from 10 am to 6 pm). The number of observation per cluster is indicated on top of the boxplots. PVSC stands for PV self-consumption and DPS for demand peak shaving.

3.4. NPV

Figure 8 shows that NPV remain negative (i.e., no profitability) in by far most cases. To put the results into perspective, the NPV can be compared to the total investment costs of the battery system (i.e., including inverter, balance of plant, installation costs and replacements to match the PV lifetime of 30 years): In Austin, in average households lose 0.83 USD per dollar invested in a battery, while in

Geneva, households lose 0.67 USD per dollar invested. However, the combination of two or more applications helps batteries to improve the economic case in both locations (see Figure 8a).

The NPV is negatively affected by and strongly dependent on the annual electricity consumption as shown in Figure 8b. The differences of the median NPV among the three consumption brackets are as high as 9200 USD in Austin, decreasing to 1400 USD in Geneva, being statistically significant in both cases (*p*-values < 0.05). Interestingly, the combination of all applications in Geneva is able reverse the negative influence of the annual electricity consumption that can be seen when PV self-consumption is the only application (see Figure 8b, right panel).

In Austin, the differences within consumption bracket and across the clusters are not statistically significant (see Figure 8c). On the other hand, batteries performing PV self-consumption only in the households with medium annual consumption in Geneva (i.e., in the range of 2025–3170 kWh) with a peak in the evening (MC1) offer higher NPV (up to 230 USD, i.e., 5%) (*p*-values < 0.05). Batteries in households with flat load profiles (LC1, MC3 and HC2), generally achieve lower NPV (differences up to 250 USD, i.e., 6%), in particular when PV self-consumption is combined with other applications. Finally, the combination of applications increases the economic viability of the batteries up to 8400 USD in Austin and 2250 USD in Geneva (*p*-values < 0.05).
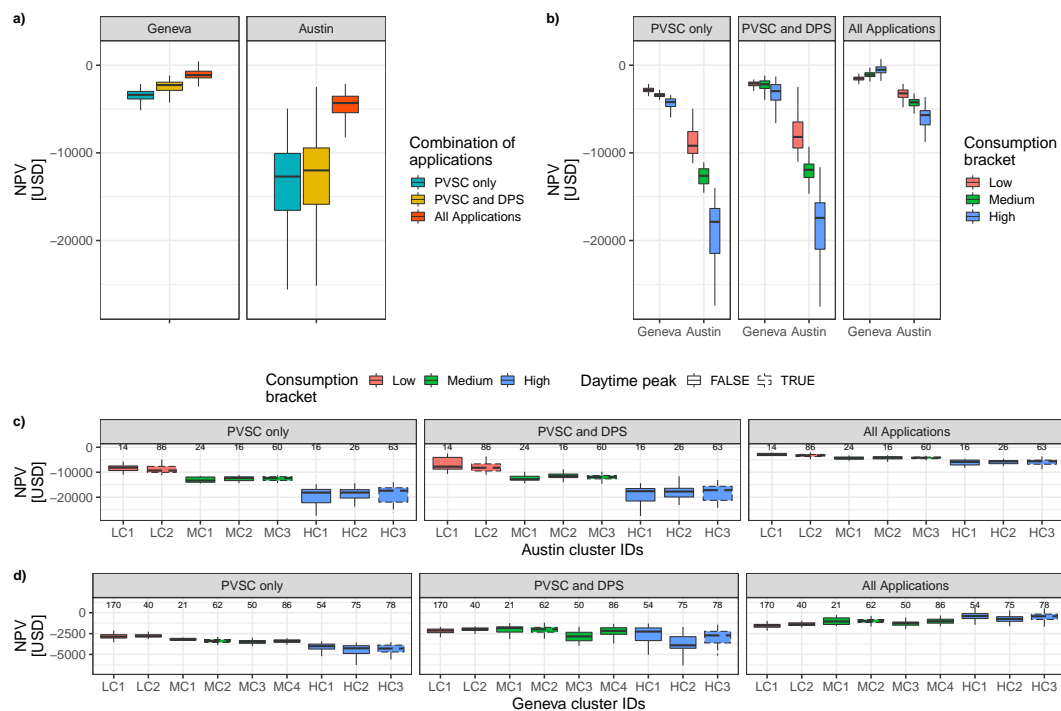

Figure 8. NPV achieved by PV-coupled batteries. (**a**) Comparing the impact of the combination of applications per country; (**b**) Comparing the consumption bracket impact per country and per combination of applications; (**c**) Comparing the impact of the load profile (cluster) per consumption bracket and per combination of applications for Austin and; (**d**) Comparing the impact of the load profile (cluster) per consumption bracket and per combination of applications for Geneva. All values presented in this graph refer only to the investment in the battery, i.e., the cost of the PV panel is excluded. Dashed boxplots represent households with peaks during daytime (i.e., from 10 a.m. to 6 p.m.). The number of observation per cluster is indicated on top of the boxplots. PVSC stands for PV self-consumption and DPS for demand peak shaving.

4. Discussion

Our results highlight the interest on the combination of applications (also called services) at the residential level and the impact of the household electricity consumption on the economic viability of installing a battery in an otherwise stand-alone PV system. They show as well the limited impact

of the load profile on the performance and economic attractiveness of PV-coupled battery systems. The results of this study are based on a 1:1:1 sizing ratio (e.g., an annual electricity consumption of 5 MWh leads to a nominal PV capacity of 5 kWp and a battery capacity of 5 kWh) [4,15].

4.1. Impact of Combination of Applications

Overall, batteries significantly increase self-consumption (ranging from 6–24%). According to our results, the combination of applications does not compromise total PV self-consumption shares or only hardly does so. We find that there are not statistically significant differences in Geneva for batteries combining applications with respect to the case of batteries performing PV self-consumption only, and in Austin we find a limited decrease of total PV self-consumption (2.6%). In turn, peak demand is positively affected by the combination of applications when PV self-consumption is combined with demand peak shaving (by up to around 20%). Interestingly, charging the battery from the grid contributes to reduce the peak flow with the grid by an additional 1.5 kW in Austin and a more modest 0.1 kW in Geneva, when compared to the combination of PV self-consumption and demand peak-shaving. The combination of applications boosts the NPV of batteries, with increases by up to 8500 USD and 2250 USD in Austin and Geneva, respectively. Combining applications leads to some positive NPV (up to 1342 USD) in households with high electricity consumption in Geneva, reversing in this way the negative impact of annual electricity consumption observed in all the other cases (a higher annual consumption implies a larger battery based on the selected sizing method). Additionally, battery applications such as demand peak-shaving and avoidance of PV curtailment provide indirect benefits to the grid operation and stability that are not captured in the NPV indicator but cannot be neglected.

A rule-of-thumb such as the 1:1:1 ratio is not reasonable for today's households with large annual consumption (e.g., Austin households) and in particular if the battery is used only for PV self-consumption. Instead, batteries should be able to combine applications to justify their large capacity and the related investment, which call for a faster deployment of policies and regulations in this direction around the globe. Further applications not included in this study should be considered, such as frequency control (e.g., within a pool of batteries controlled by a centralized organization). In households with more modest annual consumption, e.g., Swiss and other European households, the above-mentioned ratio together with the combination of applications can lead to positive economic cases, even with the current high costs of batteries (350 USD/kWh and 2000 USD for the installation). We find as well that the exclusive use of the batteries for PV self-consumption is currently not profitable without subsidies. The combination of applications and in particular the use of demand peak shaving (enabled by a capacity-based tariff) not only helps to reduce the stress on the grid but helps as well to improve battery profitability for all household types, regardless the consumption bracket or the load profile.

4.2. Impact of Electricity Annual Consumption and Load Profile

Under the sizing ratio of 1:1:1, the impact of the annual electricity demand on total PV self-consumption is small, but statistically significant (i.e., 2% in Austin and 3% in Geneva). This is also the case for the maximum peak flow exchanged with the main grid (i.e., accounting for import and export power), since higher annual electricity consumption leads to larger battery sizes and higher reductions of the peak flow as a result (compared to the case without a PV-coupled battery system) of 2.6 kW (1 kW) in Austin (Geneva. Additionally, the impact of the annual consumption on profitability is remarkable, with differences in NPV larger than 9000 USD in Austin and 1400 USD in Geneva, with large consumers being negatively affected due to the installation of larger batteries except when all applications are combined). Thus, small (or even no) battery systems should be preferred to maximize NPV in the absence of the combination of applications, due to still high capital costs [10,33]. However, larger batteries will become more affordable as battery costs progressively decline, enabling further reduction of the peak flow exchanged with the main grid.

Finally, there is a limited impact of the load profile on the performance and economic attractiveness of PV-coupled batteries combining applications. In the Swiss case, the NPV are slightly lower in households with mostly flat load profiles compared to other load profiles (6% lower NPV for clusters LC1, MC3 and HC2, see Figure 8d). Additionally, households with demand peaks in the evening (e.g., MC2 in Geneva) achieve a NPV 5% higher than when the battery is used only for PV self-consumption. On the other hand, in Austin, the load profile does not have an impact on battery profitability, which suggest that the effect of load profile differs across locations with different retail tariff values and electricity consumption thresholds.

4.3. Limitations and Future Research

Future research can apply the proposed method to analyze other locations with different electricity load profiles and retail tariff values. The grid may benefit from distributed storage in several ways, however, in this study we look at the problem from a consumer perspective. Further research regarding the potential benefits to the grid and extra remuneration mechanisms should be explored. The effect of future load profiles e.g., by better insulation of buildings (in particular in the U.S.) could also be studied. Furthermore, alternative choices of battery sizing can be explored, which may lead to different findings. In the same way, we acknowledge that a smaller value of the DoD would lead to reduced aging, however, the amount of cycles per year would also decrease and therefore the economic benefits steaming from the battery and its economic viability. Alternative values of DoD should be investigated to precisely quantify their effects on different performance indicators. Other alternatives to physical storage such as virtual storage, as applied in some countries where the grid may be used to store PV excess and may be taken back by the prosumer within a certain period of time without charge should be explored, which may reduce the prosumer investment while maintaining similar or higher shares of self-consumption. Additionally, we suggest the use of larger datasets (the Austin dataset only includes 305 households), as is the case for Geneva (with 636 households), to increase the number of observations which helps to produce results which are statistically significant.

5. Conclusions

In this study, we analyze the impact of the electricity load profile, the annual electricity consumption and the combination of applications, namely photovoltaic (PV) self-consumption, avoidance of PV curtailment, demand peak shaving, as well as demand load-shifting (with grid-charging) for PV-coupled battery systems which are sized with a 1:1:1 ratio (e.g., an annual electricity consumption of 5 MWh leads to a nominal PV capacity of 5 kWp and a battery capacity of 5 kWh). The analysis is carried out for Austin (U.S.) and Geneva (Switzerland), which have very different climates, load profiles and electricity consumption levels. Our findings rely on tests of statistical significance using 305 and 636 electricity load profiles with 15-minute resolution monitored in Austin and Geneva.

Our results indicate that the type of load profile (established by clustering) has a limited impact on the net present value (NPV) of PV-coupled batteries in Geneva. For households with mostly flat profiles, the NPV is slightly lower when combining applications compared to households with other types of load profile. Furthermore, batteries performing only PV self-consumption in households with peaks in the evening have marginally higher NPV than other households. The effect of the load profile is even less marked in Austin where we find practically no impact of the load profile on demand peak shaving and NPV in Austin, while total PV self-consumption is positively affected in households with daytime peaks. In conclusion, the type of load profile has a relatively small influence on the techno-economic attractiveness of PV-coupled battery systems, but this conclusion should be tested also for other locations.

If confirmed, the value of PV-coupled battery systems is not increased by tariffs which are customized to the load profile of consumers based on our results.

Furthermore, we find that the NPV of batteries benefits most from combining applications, regardless of the annual electricity consumption level, load profile and location. Interestingly, the total PV self-consumption rate of PV-coupled batteries is not compromised by the inclusion of other applications beyond PV self-consumption. This finding confirms that batteries should be used for multiple applications, which in turn needs regulatory changes. For instance, the inclusion of capacity-based tariff sends a signal to reduce peak demand. This offers synergies for consumers who increase the value of their batteries and distribution system operators who reduce grid stress. This conclusion is important for the economic viability of batteries, which are crucial to support further PV penetration.

Author Contributions: Conceptualization, D.P. and A.P.-B.; investigation, A.P.-B.; methodology, A.P.-B., D.P. and E.B.; software, A.P.-B., E.B., M.C.G. and S.Y.; formal analysis, A.P.-B.; validation, E.B. and S.Y.; writing—original draft, A.P.-B.; writing—reviewing and editing, E.B., M.C.G., S.Y., M.K.P. and D.P.; supervision, M.K.P. and D.P. All authors have read and agreed to the published version of the manuscript.

Conflicts of Interest: The authors declare no conflict of interest.

Abbreviations

The following abbreviations are used in this manuscript:

PV	Photovoltaics
FiT	Feed-in Tariff
PVSC	PV self-consumption
PVCT	Avoidance of PV curtailment
DLS	Demand load-shifting
DPS	Demand peak shaving
NMC	Lithium nickel manganese cobalt oxide
ILR	Inverter load ratio
ToU	Time of use
NPV	Net present value
CF	Cash flow
SOC	State of charge
DoD	Depth of discharge

References

1. IRENA. *Electricity Storage and Renewables: Costs and Markets to 2030*; International Renewable Energy Agency: Abu Dhabi, UAE, 2017.
2. Kavlak, G.; McNerney, J.; Trancik, J.E. Evaluating the causes of cost reduction in photovoltaic modules. *Energy Policy* **2018**, *123*, 700–710. [CrossRef]
3. California Public Utilities Commission. *Self-Generation Incentive Program*; California Public Utilities Commission: San Francisco, CA, USA, 2017.
4. Weniger, J.; Tjaden, T.; Quaschning, V. Sizing of Residential PV Battery Systems. *Energy Procedia* **2014**, *46*, 78–87. [CrossRef]
5. Luthander, R.; Widen, J.; Munkhammar, J.; Lingfors, D. Self-consumption enhancement and peak shaving of residential photovoltaics using storage and curtailment. *Energy* **2016**, *112*, 221–231. [CrossRef]
6. Pena-Bello, A.; Burer, M.; Patel, M.K.; Parra, D. Optimizing PV and grid charging in combined applications to improve the profitability of residential batteries. *J. Energy Storage* **2017**, *13*, 58–72. [CrossRef]

7. Truong, C.N.; Naumann, M.; Karl, R.C.; Müller, M.; Jossen, A.; Hesse, H.C. Economics of Residential Photovoltaic Battery Systems in Germany: The Case of Tesla's Powerwall. *Batteries* **2016**, *2*, 14. [CrossRef]

8. Hesse, H.C.; Martins, R.; Musilek, P.; Naumann, M.; Truong, C.N.; Jossen, A. Economic Optimization of Component Sizing for Residential Battery Storage Systems. *Energies* **2017**, *10*, 835. [CrossRef]

9. Magnor, D.; Sauer, D.U. Optimization of PV battery systems using genetic algorithms. *Energy Procedia* **2016**, *99*, 332–340. [CrossRef]

10. Barbour, E.; González, M.C. Projecting battery adoption in the prosumer era. *Appl. Energy* **2018**, *215*, 356–370. [CrossRef]

11. Schopfer, S.; Tiefenbeck, V.; Staake, T. Economic assessment of photovoltaic battery systems based on household load profiles. *Appl. Energy* **2018**, *223*, 229–248. [CrossRef]

12. Linssen, J.; Stenzel, P.; Fleer, J. Techno-economic analysis of photovoltaic battery systems and the influence of different consumer load profiles. *Appl. Energy* **2017**, *185*, 201–2025. [CrossRef]

13. O'Shaughnessy, E.; Cutler, D.; Ardani, K.; Margolis, R. Solar plus: A review of the end-user economics of solar PV integration with storage and load control in residential buildings. *Appl. Energy* **2018**, *228*, 2165–2175. [CrossRef]

14. Ratnam, E.L.; Weller, S.R.; Kellett, C.M. An optimization-based approach to scheduling residential battery storage with solar PV: Assessing customer benefit. *Renew. Energy* **2015**, *75*, 123–134. [CrossRef]

15. Litjens, G.; Worrell, E.; van Sark, W. Assessment of forecasting methods on performance of photovoltaic-battery systems. *Appl. Energy* **2018**, *221*, 358–373. [CrossRef]

16. Beck, T.; Kondziella, H.; Huard, G.; Bruckner, T. Assessing the influence of the temporal resolution of electrical load and PV generation profiles on self-consumption and sizing of PV-battery systems. *Appl. Energy* **2016**, *173*, 331–342. [CrossRef]

17. Chicco, G. Overview and performance assessment of the clustering methods for electrical load pattern grouping. *Energy* **2012**, *42*, 68–80. [CrossRef]

18. Kwac, J.; Flora, J.; Rajagopal, R. Household energy consumption segmentation using hourly data. *IEEE Trans. Smart Grid* **2014**, *5*, 420–430. [CrossRef]

19. Xu, S.; Barbour, E.; González, M.C. Household segmentation by load shape and daily consumption. *Proc. ACM SigKDD* **2017**, *2*, 1–9.

20. Benítez, I.; Quijano, A.; Díez, J.L.; Delgado, I. Dynamic clustering segmentation applied to load profiles of energy consumption from Spanish customers. *Int. J. Electr. Power Energy Syst.* **2014**, *55*, 437–448. [CrossRef]

21. Al-Wakeel, A.; Wu, J.; Jenkins, N. K-means based load estimation of domestic smart meter measurements. *Appl. Energy* **2017**, *194*, 333–342. [CrossRef]

22. Tureczek, A.; Nielsen, P.S.; Madsen, H. Electricity consumption clustering using smart meter data. *Energies* **2018**, *11*, 859. [CrossRef]

23. Yilmaz, S.; Chambers, J.; Patel, M.K. Comparison of clustering approaches for domestic electricity load profile characterisation-Implications for demand side management. *Energy* **2019**, *180*, 665–677. [CrossRef]

24. Räsänen, T.; Kolehmainen, M. Feature-based clustering for electricity use time series data. In *International Conference on Adaptive and Natural Computing Algorithms*; Springer: Berlin/Heidelberg, Germany, 2009, pp. 401–412.

25. Bellman, R.E. *Adaptive Control Processes: A Guided Tour*; Princeton University Press: Princeton, NJ, USA, 2015.

26. Haben, S.; Singleton, C.; Grindrod, P. Analysis and clustering of residential customers energy behavioral demand using smart meter data. *IEEE Trans. Smart Grid* **2015**, *7*, 136–144. [CrossRef]

27. Rousseeuw, P.J. Silhouettes: a graphical aid to the interpretation and validation of cluster analysis. *J. Comput. Appl. Math.* **1987**, *20*, 53–65. [CrossRef]

28. Parra, D.; Walker, G.S.; Gillott, M. Modeling of PV generation, battery and hydrogen storage to investigate the benefits of energy storage for single dwelling. *Sustain. Cities Soc.* **2014**, *10*, 1–10. [CrossRef]

29. Sanyo Electric Co., Ltd. *HIT Photovoltaic Module HIT-N2XXSE10 Datasheet*; Sanyo Electric: Osaka, Japan, 2018

30. Burger, B.; Rüther, R. Inverter sizing of grid-connected photovoltaic systems in the light of local solar resource distribution characteristics and temperature. *Solar Energy* **2006**, *80*, 32–45. [CrossRef]

31. Baumann, T.; Baumgartner, F. *Home Batteriespeicher, Studie für Solarspar*; Technical report; ZHAW/IEFE: Winterthur, Switzerland 2017.

32. ITP Renewables. *Battery Test Centre - Public Report 1*; Technical report; Lithium Ion Battery Test Centre Program: Canberra, Australia 2016.

33. Pena-Bello, A.; Barbour, E.; Gonzalez, M.; Patel, M.; Parra, D. Optimized PV-coupled battery systems for combining applications: Impact of battery technology and geography. *Renew. Sustain. Energy Rev.* **2019**, *112*, 978–990. [CrossRef]

34. Victron Energy *EasySolar 12/1600/70*; Victron Energy: Almere, The Netherlands, 2017.

35. Ardani, K.; O'Shaughnessy, E.; Fu, R.; McClurg, C.; Huneycutt, J.; Margolis, R. *Installed Cost Benchmarks and Deployment Barriers for Residential Solar Photovoltaics with Energy Storage: Q1 2016*; Technical report; NREL (National Renewable Energy Laboratory (NREL): Golden, CO, USA, 2016.

36. Fu, R.; Feldman, D.J.; Margolis, R.M.; Woodhouse, M.A.; Ardani, K.B. *US Solar Photovoltaic System Cost Benchmark: Q1 2017*; Technical report; National Renewable Energy Laboratory (NREL): Golden, CO, USA, 2017.

37. Tesla Inc. *Powerwall 2 DC*; Tesla Inc.: San Carlos, CA, USA, 2019.

38. Stephan, A.; Battke, B.; Beuse, M.D.; Clausdeinken, J.H.; Schmidt, T.S. Limiting the public cost of stationary battery deployment by combining applications. *Nat. Energy* **2016**, *16079*. [CrossRef]

39. Käbitz, S.; Gerschler, J.B.; Ecker, M.; Yurdagel, Y.; Emmermacher, B.; André, D.; Mitsch, T.; Sauer, D.U. Cycle and calendar life study of a graphite∣LiNi1/3Mn1/3Co1/3O2 Li-ion high energy system. Part A: Full cell characterization. *J. Power Sour.* **2013**, *239*, 572–583. [CrossRef]

40. Parra, D.; Patel, M.K. The nature of combining energy storage applications for residential battery technology. *Appl. Energy* **2019**, *239*, 1343–1355. [CrossRef]

41. AEMC. *2014 Residential Electricity Price Trends*; Australian Energy Market Commission (AEMC): Sydney, Australia, 2014.

42. Hart, W.E.; Laird, C.; Watson, J.P.; Woodruff, D.L. *Pyomo-optimization Modeling in Python*; Springer: Berlin/Heidelberg, Germany, 2012; Volume 67.

43. Parra, D.; Norman, S.A.; Walker, G.S.; Gillott, M. Optimum community energy storage system for demand load shifting. *Appl. Energy* **2016**, *174*, 130–143. [CrossRef]

44. Moore, M.; Counce, R.; Watson, J.; Zawodzinski, T. A Comparison of the Capital Costs of a Vanadium Redox-Flow Battery and a Regenerative Hydrogen-Vanadium Fuel Cell. *J. Adv. Chem. Eng.* **2015**, *5*, 3.